Controlled *p*-type doping of polycrystalline and amorphous organic layers: Self-consistent description of conductivity and field-effect mobility by a microscopic percolation model

B. Maennig, M. Pfeiffer, A. Nollau, X. Zhou, and K. Leo
Institut für Angewandte Photophysik, Technische Universität Dresden, D-01062 Dresden, Germany

P. Simon
Institut für Angewandte Physik und Didaktik der Physik, Technische Universität Dresden, D-01062 Dresden, Germany
(Received 24 April 2001; published 22 October 2001)

We present a systematic study on *p*-type doping of zinc-phthalocyanine by tetrafluoro-tetracyano-quinodimethane as an example of controlled doping of thin organic films by cosublimation of matrix and dopant. The zinc-phthalocyanine layers are prepared both in polycrystalline and amorphous phase by variation of the sublimation conditions. The films are electrically characterized *in situ* by temperature dependent conductivity and Seebeck and field-effect measurements. In addition to previous work, we show that also amorphous phthalocyanine layers can be doped, i.e., their conductivity increases and their Seebeck coefficient decreases indicating a shift of the Fermi level towards the hole transport level. The field-effect mobility of the polycrystalline samples is in the range of 10^{-4}–10^{-3} cm^{-2}/Vs and increases with increasing dopant concentration. Adapting a percolation model presented by Vissenberg and Matters [Phys. Rev. B, **57**, 12 964 (1998)], which assumes hopping transport within a distribution of localized states, we can quantitatively describe the conductivity (in different organic layers) and the field-effect mobility.

DOI: 10.1103/PhysRevB.64.195208 PACS number(s): 73.50.Lw, 73.61.Jc, 73.50.Dn

I. INTRODUCTION

Thin films of organic dyes with conjugated π-electron systems are widely investigated for use in electronic and optoelectronic devices like organic light emitting diodes, field-effect transistors and solar cells.[1–7] Although it is known for a long time that the conductivity of organic layers can be enhanced remarkably by coevaporation with strong organic π-electron donors or acceptors,[8–10] organic devices are usually prepared in a nominally undoped form. However, the electrical properties of undoped layers are governed by unknown impurities or by gases such as oxygen.[7,11,12] Schön *et al.* presented the doping of pentacene and α-hexathiophene single crystals with iodine reaching a conductivity up to 10^{-3} S/cm.[13] The history of silicon technology showed that controlled doping is necessary for the realization of effective, stable and reproducible devices: The breakthrough of classical microelectronics became possible due to the preparation of materials with high purity and controlled doping levels. Recently, we also showed that the properties of *organic* devices such as light emitting diodes (OLED's) and organic solar cells are strongly improved by controlled doping.[14–16]

Organic dye layers are typically prepared by vapor deposition in high vacuum or spin coating from solution and have a polycrystalline or amorphous morphology. Amorphous materials are in particular popular for OLED's, mainly because they form smooth layers and do not degrade by crystallization (if the glass transition temperature is high enough). However, only a few attempts are reported to dope amorphous layers by coevaporation.[14,16] To our knowledge, no results are reported about the dependence of the morphology of the matrix on the doping efficiency.

The doping process (in polycrystalline dyes) can largely be described by the standard model used for crystalline anorganic semiconductors.[17,18] However, a proper thermodynamic description of the doping process is still a challenge. In particularly, the strong superlinear increase of the conductivity with doping observed in some systems calls for an explanation.[19] One problem for the description is the polycrystalline morphology of the layers: It is not known whether the current flows primarily through the grains or along the grain boundaries. Furthermore, it is not known whether the dopants are homogeneously distributed in the material or if they are diffused out of the grains and concentrate at the grain surfaces. In this respect, amorphous materials are more simple model systems.

Here, we report on our investigation on the semiconducting behavior of polycrystalline and amorphous vacuum deposited layers, intentionally *p* doped with a strong acceptor molecule. We chose zinc-phthalocyanine (ZnPc) as a model matrix material and tetrafluoro-tetracyano-quinodimethane (F_4-TCNQ) as dopant because the doping process is quite efficient for these two materials.[19] Polycrystalline and amorphous ZnPc films were prepared by variation of the substrate temperature during layer growth. The films are electrically characterized by temperature dependent measurements of the conductivity, the thermopower (Seebeck effect) and the field-effect mobility. From the Seebeck coefficient, we can calculate the hole density p. In combination with the measured conductivity σ, we obtain the hole mobility μ_h (assuming $\sigma = ep\mu_h$). The field-effect measurements allow us directly to determine the hole mobility and to compare the values. The results for μ_h obtained from the different measurements are largely consistent. We will show that a comprehensive

 ©2001 The American Physical Society

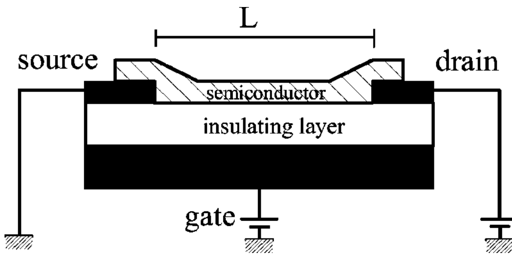

FIG. 1. Schematic view of a thin film transistor (TFT): The channel length L is 300 μm, the thickness and the capacitance C_i of the insulating layer, respectively are 50 nm and 60nF/cm^2 for SiO_2 and 1μm and 1nF/cm^2 for Benzo Cyclo Butene.

description requires a percolation model both for polycrystalline and amorphous materials.

II. EXPERIMENT

ZnPc was delivered by Syntec GmbH (Wolfen, Germany). The material was purified by vacuum gradient sublimation. F_4-TCNQ was used as provided by Aldrich. The samples were prepared in a high vacuum chamber (4×10^{-4} Pa). The matrix and the dopant were coevaporated from graphite and ceramic crucibles, respectively, using 1.63 g/cm^3 as density of ZnPc. For the conductivity and Seebeck-measurements, the films were grown onto precleaned fused silica substrates. The morphology of the films depended on the temperature of the substrates, as known for CuPc:[20] A polycrystalline film (α-phase) grew when the substrate was held at room temperature (RT samples) and an almost amorphous film when the substrate was cooled down to at least $-100\,^\circ$C (LT samples). We found this behavior for different substrate materials such as silica, KBr, and carbon foil. The amorphous phase was stable up to 50 °C.

The morphology of ZnPc was analyzed by electron diffraction using a transmission electron microscope Philips CM200 LaB_6. Here, Cu-grids coated with a carbon foil (Plano W. Plannet GmbH, S160-3) were used as substrate and the ZnPc layers were 50 nm thick. For the conductivity and Seebeck measurements, the fused silica substrates were already equipped with two vapor-deposited gold contacts with a distance of 2 mm. Here, the thickness of the ZnPc layers was 30 nm. The samples show linear current-voltage characteristics. Due to the high resistance of the organic layers, the electrical properties are determined by the bulk material and not by the contacts. The conductivity and Seebeck coefficient were recorded with a source measure unit (Keithley SMU236). The polycrystalline samples were annealed in vacuum at 70 °C for 30 min and the amorphous samples at 50 °C for 30 min before the measurements. Details of the sample preparation and the conductivity and Seebeck-measurements are described in Ref. 14.

The field-effect mobility was determined with thin film transistors (Fig. 1). We used two types of samples. The first one (type I) consists of a silicon oxide insulating layer (50 nm thick) thermally grown on a highly doped *n*-type silicon wafer. Onto the oxide layer, the source and drain gold electrodes (25 nm thick) were deposited with a channel length and width of 300 μm and 8 mm, respectively. Finally, the ZnPc layer (30 nm thick) was deposited. The second type of samples (type II) is based on a commercially available indium-tin-oxide-layer (ITO) on a glass substrate. The insulating polymer BCB (Benzo Cyclo Butene, Cyclotene 3022, DOW Chemical Company) was deposited by spin coating. The thickness of the polymer is about 1 μm and the resistivity around 10^{16} Ω cm. Then, the gold electrodes and the ZnPc layer were deposited in the same way. Current voltage characteristics were obtained with the source measure unit; to apply the gate voltage, we used an electrometer (Keithley, 617 Programmable Electrometer). All electrical measurements presented here were carried out *in situ*.

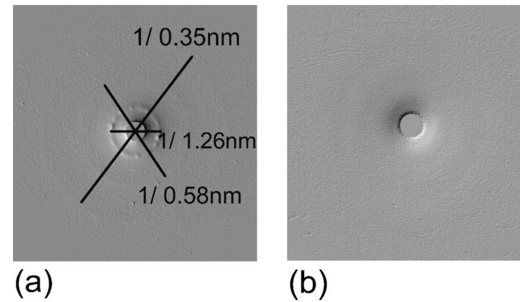

FIG. 2. Differentiated diffraction images of two ZnPc layers (50 nm thick) on a carbon foil: The layers were prepared at a substrate temperature of (a) 25 °C and (b) $-150\,^\circ$C. The original (not differentiated) diffraction images are hard to analyze because of the very low intensity. The numbers in (a) declare the distance in nm of the corresponding crystallographic planes.

III. RESULTS AND DISCUSSION

A. Structural characterization

Two types of ZnPc samples were prepared: The room temperature (RT) sample was prepared while the substrate was held at room temperature (25 °C). The low temperature (LT) sample was prepared while the substrate was cooled to $-150\,^\circ$C. The differentiated diffraction patterns of the RT and LT samples are shown in Fig. 2. The RT sample shows sharp Debye Scherrer rings and some discrete diffraction spots due to the polycrystalline morphology of the phtalocyanine [Fig. 2(a)]. The rings correspond to the (200), (40-2), and (31-2) lattice planes. These planes represent lattice spacings of 1.26, 0.58, and 0.35 nm of the low temperature α-phase crystalline modification of ZnPc. The crystalline domains have an average size of about 20–30 nm. In the diffraction pattern of the LT sample, the Debye-Scherrer rings are missing. Only amorphous halos corresponding to 1.26, 0.58, and 0.35 nm can be observed. The amorphous phase is stable up to a temperature of 50 °C. Above this value, the films recrystallize (α phase).

The absorption spectra of the RT and LT samples are shown in Fig. 3. Absorption spectra of ZnPc in solution shows only one peak at 679 nm in the depicted energy range.[19,21] In the solid state, this electronic excitation splits up in two parts because of the molecular interactions (see Ref. 22). The positions of the peaks are 625 and 710 nm for

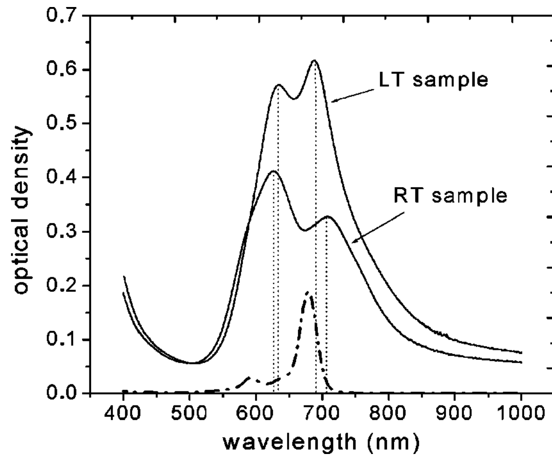

FIG. 3. Absorption spectra of ZnPc layers (50 nm thick): The RT sample was prepared at 25 °C substrate temperature and the LT sample at −150 °C substrate temperature. The dotted spectra shows schematically the absorption of ZnPc dissolved in 1-chloronaphthaline.

the RT sample and 635 and 688 nm for the LT sample, respectively. The separation of the peaks is smaller for the amorphous than for the polycrystalline phase. This is a strong hint at a lower interaction of the molecules of the LT sample, which fits well with the lower degree of order.

B. Conductivity and Seebeck coefficient

The conductivity of undoped ZnPc is below 10^{-10} S/cm. The conductivity σ versus the reciprocal temperature for the doped samples grown at different substrate temperature is plotted in Fig. 4(a). The molar dopant concentration is 1 % in both samples. At room temperature, the conductivity is six orders of magnitude higher than in the undoped samples. The conductivity shows a thermally activated behavior in the measured temperature range. For the RT sample the activation energy is $E_{\mathrm{act}}=0.18$ eV. In comparison, the activation energy is $E_{\mathrm{act}}=0.24$ eV for a molar dopant concentration of 0.2 %, i.e., the activation energy slightly decreases with increasing dopant concentration. For the LT sample the activation energy is 0.23 eV. Again, the activation energy is higher for a molar dopant concentration of 0.2 % (0.29 eV).

Figure 4(b) shows the conductivity vs the molar doping ratio. Surprisingly, the conductivity increases strongly superlinearly with the concentration of F_4-TCNQ for both types of samples. Generally, the conductivity of the LT samples is about one order of magnitude lower compared to the RT samples. The conductivity of the RT sample with the lowest molar doping ratio (0.063 %) is smaller than one would expect from the curve of the other samples. For a molar doping concentration of 0.033 %, we were not even able to measure any current ($\sigma<10^{-10}$ S/cm). This is a strong hint at the influence of impurities in the matrix: The charge carriers are trapped in the impurity states and the conductivity is significantly lowered as long as the density of traps is in the same order or even higher as the density of dopants. This effect can be neglected if the doping concentration is much higher than the trap density.

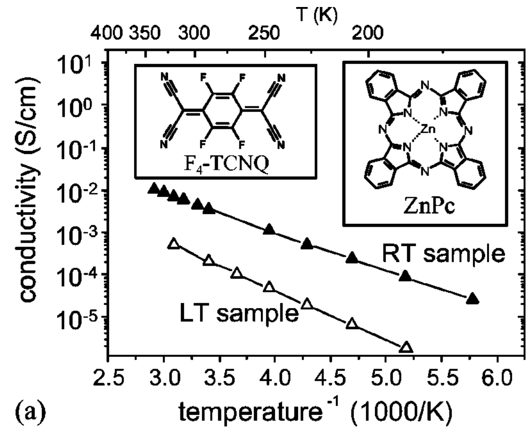

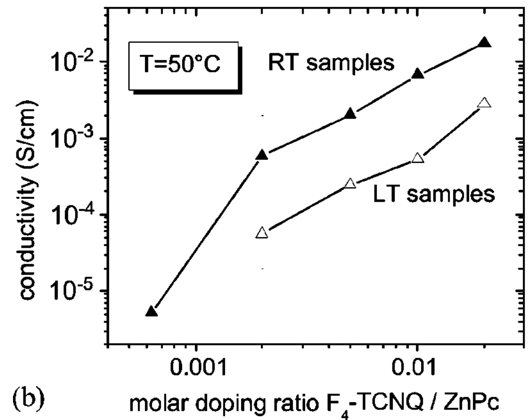

FIG. 4. Conductivity of ZnPc layers (30 nm thick) doped with F_4-TCNQ: (a) Arrhenius plot for a RT and LT sample with a molar doping ratio of 1%; The insets show the structures of matrix (ZnPc) and doping (F_4-TCNQ) molecules. (b) Conductivity vs molar doping ratio for the RT and LT samples: The conductivity of the LT samples is about one order of magnitude lower compared to the RT samples.

The Seebeck coefficient S is defined as

$$S(T)=\lim_{\Delta T\to 0}\frac{U_{12}(T,\Delta T)}{\Delta T}, \tag{1}$$

where T is the absolute temperature, U_{12} the thermovoltage between the contacts 1 and 2 and ΔT the temperature difference between the contacts 2 and 1. For a first analysis, we use the standard model of only one relevant transport level. We will later see that this standard model cannot completely explain our measurements. For unipolar charge carrier transport *at one transport level* E_μ, S is given by[23]

$$S(T)=\frac{E_F(T)-E_\mu}{eT}. \tag{2}$$

Equation (2) shows that the Seebeck coefficient S reveals the transport type (n or p) from its sign and the energetic difference between the Fermi level E_F and the relevant transport level E_μ from its value. It is important to mention that Eq. (2) holds regardless of the details of the transport mecha-

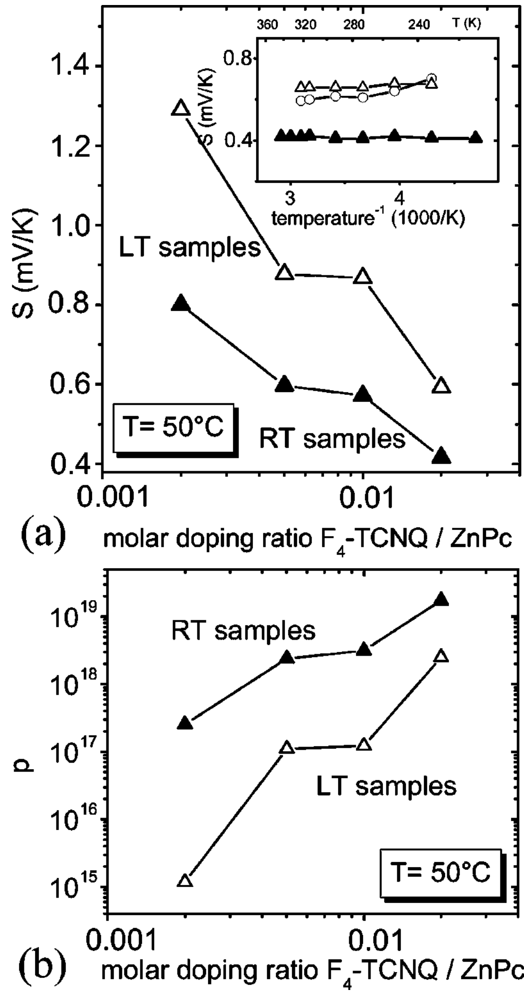

FIG. 5. (a) Seebeck coefficient S vs molar doping ratio for ZnPc layers (30 nm thick) doped with F_4-TCNQ: The values of the LT samples are about 0.2–0.3 mV/K higher than for the RT samples. The inset shows the Seebeck coefficient vs temperature for a RT and LT sample with a molar doping ratio of 2% and a 400 nm thick LT sample with a molar doping ratio of 1.2%. Here, the slightly increase of S with 1/T for the thin LT sample (open circle) is due to problems of the measurement because of the low current in the thin film. For the thicker layer (open triangle) S stays constant. (b) Hole density vs molar doping ratio.

nism. For instance, it applies to band transport (as long as the band width is small compared to kT), and to hopping transport.[23]

All Seebeck coefficients S we measure are positive [Fig. 5(a)]. This means that the conduction is due to holes moving in the valence states of the matrix molecules and not by a hopping of electrons between acceptor states. With increasing doping, the value of the coefficient gets smaller, i.e., the difference between the transport level and the Fermi level becomes smaller. If we assume that the transport levels stay at the same energy, the behavior seems to follow the situation in inorganic semiconductors: With increasing doping, the Fermi level E_F shifts towards the transport level E_μ. The Seebeck coefficient S of the LT samples is about 0.2–0.3 mV/K higher than for the RT samples. For all samples, S is basically temperature independent [see inset of Fig. 5(a)].

For the further evaluation of the Seebeck measurements, we assume that the effective density of states N_μ at the transport level E_μ is comparable to the density of molecules N_m. This is equivalent to the assumption that every molecule contributes one transport state. For α-ZnPc, the density of molecules is about $N_m = 1.7\times 10^{21}$ cm^{-3}. The density of (free) holes p in the transport state is then given by

$$p = N_\mu \exp\left(-\frac{E_F(T)-E_\mu}{k_B T}\right) = N_\mu \exp\left(-\frac{eS}{k_B}\right) \tag{3}$$

with k_B as the Boltzmann constant. We can use here the Maxwell-Boltzmann approximation since $E_F - E_\mu \gg k_B T$. Note that the effective density of states N_μ is not known in our materials and that for a comprehensive understanding of the measurements one has to go beyond the assumption of only one relevant transport level (see percolation model). Therefore the values of the hole density determined this way from the Seebeck coefficient are an upper limit because the effective density of states will always be lower than the density of molecules ($N_\mu \leqslant N_m$). The combination of the Seebeck measurements with the conductivity results then allows us to deduce the hole mobility by applying the equation

$$\sigma = e p \mu_h . \tag{4}$$

The obtained hole density range from 10^{15} to 10^{19} cm^{-3} [Fig. 5(b)]. They show the same characteristic behavior upon doping as the conductivity: The hole density increases strongly superlinearly with the concentration of F_4-TCNQ and the values for the LT samples are about one order of magnitude lower than for the RT samples. As a result, the hole mobility is independent of the doping density and has the same value of about 5×10^{-3} cm^2/Vs at room temperature for the RT and LT samples. Altogether, we obtain qualitatively the same behavior for the RT and the LT samples upon doping. It is therefore very unlikely that the superlinear increase of the conductivity with doping is caused by structural effects such as high conductance paths or an accumulation of F_4-TCNQ molecules at grain boundaries. Such structural effects are not expected in an amorphous phase. Accordingly, they should be much more pronounced in the RT samples than in the LT samples which are largely amorphous.

The (free) hole density appears to be temperature independent because the Seebeck coefficient is temperature independent. To explain this temperature behavior in the standard model, we would have to assume that the acceptors form shallow states, i.e., all acceptors are ionized, and that there are only shallow traps (or no traps).[19] In any other case, p increases with temperature. However, in this situation the hole density and the conductivity should increase linearly with the doping density, which is in clear contradiction to our measurements. To understand this phenomenon, we will first consider the evolution of the field-effect mobility upon doping.

C. Field effect

It is common to use the basic equations of the silicon-based MISFET (metal-insulator-semiconductor field-effect transistor) to describe the organic-based TFT (thin film transistor) although the device structure of the organic TFT's differs from that of the conventional MISFET's.[4,24,25] The drain current I_D is then given by

$$I_D = \frac{Z}{L}\mu_{\mathrm{FE}}C_i\left[(V_G - V_{\mathrm{th}})V_D - \frac{1}{2}V_D^2\right] \tag{5}$$

for $V_D < V_G - V_{\mathrm{th}}$. Here, Z is the width of the source and drain electrodes, L is the channel length, μ_{FE} is the field-effect mobility, C_i is the capacitance per unit area of the insulating layer, V_G and V_D are the applied gate and drain voltage, and V_{th} is the threshold voltage. The field-effect mobility is an effective mobility, which is related to the mobility μ_h of the holes by

$$\mu_{\mathrm{FE}} = \mu_h \frac{p}{p + p_t} \tag{6}$$

in the standard model of only one relevant transport level for a *p*-type semiconductor. Here, p is the free hole density, p_t the density of trapped holes, and μ_h is the mobility of free holes. The transfer characteristics of the thin film transistor is given in Fig. 6(a) for a RT sample. The drain current changes between 700 and 950 nA by varying the gate voltage between $+10$ and -10 V. The output characteristics are completely in the linear regime. The drain current can not be reduced to zero because the density of the induced charge carriers ($p_{\mathrm{ind}} = CV_G/e \approx 1.2\times10^{18}$ cm^{-3} for $V_G = 10V$) is only in the order of 35% of the hole density ($p \approx 3\times10^{18}$ cm^{-3}) for a molar doping ratio of 0.7%. Additionally, the depletion width ($l_{\mathrm{dep}} \approx 8$ nm) is smaller than the thickness of the ZnPc layer (30 nm) so that the layer can not be completely depleted. We use 30 nm thick ZnPc layers because films with a thickness of less than 20 nm do not form a compact layer. The doping ratio is indeed too high to produce a device with a high on/off ratio. However, our aim is not to obtain good FET characteristics, here, but to study the effect of doping on the electrical properties of the organic layers.

As the threshold voltage V_{th} is unknown, the field-effect mobility can be best calculated from the slope of the curves in the transfer characteristics

$$\frac{dI_D}{dV_G} = \frac{Z}{L}\mu_{\mathrm{FE}}C_iV_D. \tag{7}$$

For a drain voltage of -5 V, we obtain $\mu_{\mathrm{FE}} = 7\times10^{-4}$ cm^{-3} at 20 °C. This is a typical value for ZnPc and other polycrystalline organic materials.[20,26,27] The values of the field-effect mobility for the RT samples determined for thin film transistors of type I and type II are given in Fig. 6(b). Up to now, we could not obtain FET data for the LT samples. For the thin film transistors of type I and type II, the values are in the same range with a deviation of 50%, which is probably due to the different growth behavior of ZnPc on different substrates. The field-effect mobility increases with

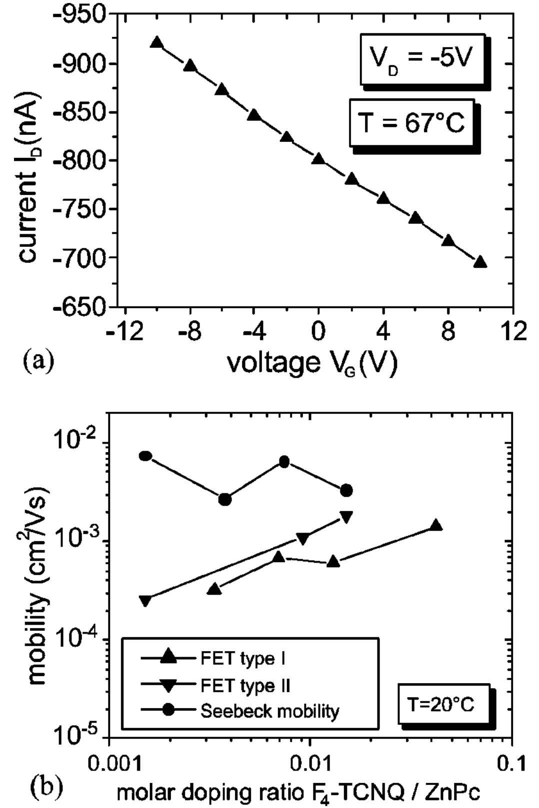

FIG. 6. (a) Transfer characteristic of a thin film transistor (type I) using a 30 nm polycrystalline ZnPc layer as active semiconductor (doping ratio 0.7%). (b) Field-effect mobility and Seebeck-mobility (definition see text) vs molar doping ratio: The field-effect mobility increases with increasing dopant concentration and the Seebeck-mobility seems to be independent of the doping concentration (within the experimental error).

increasing dopant concentration. This effect can be explained in the following way: The measured field-effect mobility is the mobility of the charge carriers additionally induced by the gate voltage. With increasing doping concentration, the traps in the material become gradually filled. As a result, the additionally induced charge carriers have a smaller probability to be trapped. The effective mobility increases according to Eq. (6) because the ratio of p and p_t increases.

The field-effect mobility shows a thermally activated behavior with the same activation energy as the conductivity. This is a strong hint for shallow acceptor states, because it implies that the total hole density $p + p_t = \sigma/\mu_{\mathrm{FE}}e$ is temperature independent. For comparison, the mobility derived from the combination of the Seebeck and conductivity measurements, which will be denoted as Seebeck-mobility μ_{SE} in the following, is also given in Fig. 6(b). The Seebeck-mobility seems to be independent of the doping concentration (within the experimental error) and is about a factor of 5 higher than the field-effect mobility at high doping ratios. The Seebeck-mobility and the field-effect mobility are thus in the same order of magnitude. The assumption that the effective hole density N_μ is equal to the density of molecules appears therefore realistic. The Seebeck-mobility is equal to the mobility of *free* holes [Eq. (6)] and therefore must be

higher than the field-effect mobility. A comparison of Seebeck and field-effect mobility allows an estimate of the hole trap density p_t: From Eq. (6) we can estimate $p_t = 1-3 \times 10^{19}\ \mathrm{cm}^{-3}$ for high doping concentrations.

D. Percolation model

With the standard semiconductor model used above, we can either explain the superlinear increase of the conductivity upon doping (by a partial trap filling) *or* the temperature independence of the hole density (by shallow acceptors and shallow traps), but not both together. For a comprehensive understanding of the measurements, we have to go beyond the assumption of only one relevant transport level. In disordered organic materials, the polarization energy of a charge carrier is different at different places. Therefore, it is more realistic to assume a distribution of localized states. The distribution is typically a Gaussian for an amorphous material. The charge transport is governed by hopping, for example, thermally activated tunneling between the localized states, in the tail of the Gaussian distribution and not by the activation of carriers to a fixed transport level. In this model, a superlinear increase of the conductivity upon doping is easy to explain: At higher dopant concentrations, more states within the distribution are filled with charge carriers (i.e., the Fermi level is higher) and the transport takes place at higher energy levels. Here, the concentration of states and consequently the hopping rate for charge carriers is higher.

To determine the conductivity of such a system, one can use the percolation theory regarding the system as a random resistor network (network of Miller and Abrahams).[29,30] The classical percolation problem considers the current flow through "bonds" connecting "sites" in a network. The conductance between the sites m and m' is given by

$$Z_{mm'}^{-1} = Z_0^{-1} \exp(-2\alpha|\vec{R}_m - \vec{R}_{m'}|) \times \exp\left(-\frac{|E_m - E_F| + |E_{m'} - E_F| + |E_{m'} - E_m|}{2kT}\right). \quad (8)$$

Here, Z_0^{-1} is a prefactor, α^{-1} the Bohr radius of the localized wave functions, which are assumed to be s-like, $\vec{R}_m$ denotes the position of the mth site, and E_m is the energy of the charge carriers at site m. The first part of Eq. (8) is a tunneling term and the second a thermal activation term (Boltzmann term). For the calculation, the resistors $Z_{mm'}$ are all removed from the network and after that replaced one by one, the smallest first.[29] The value of $Z_{mm'}$ at which the first infinite cluster occurs is Z_c, the *threshold* or *critical* value. This critical value determines the conductivity of the system:

$$\sigma = \sigma_0 Z_c^{-1}. \quad (9)$$

Here, σ_0 is a prefactor. To describe our measurements, we adapt a model by Vissenberg and Matters, which originally describes the field-effect mobility in amorphous organic transistors.[1] It assumes the following exponential density of localized states (for electrons in the conduction states):

$$g(E) = \frac{N_t}{k_B T_0} \exp\left(\frac{E}{k_B T_0}\right). \quad (10)$$

Here, N_t is the number of states per unit volume and T_0 describes the width of the exponential distribution. Vissenberg and Matters point out that they do not expect the results to be qualitatively different for a different choice of $g(E)$, as long as $g(E)$ increases strongly with E. Therefore, we can use their results assuming that the transport takes place in the tail of a Gaussian distribution. Combining Eqs. (8)–(10), Vissenberg and Matters obtain the following equation for the conductivity:

$$\sigma(\delta, T) = \sigma_0 \left(\frac{\pi \delta N_t (T_0/T)^3}{(2\alpha)^3 B_C \Gamma(1 - T_0/T) \Gamma(1 + T_0/T)}\right)^{T_0/T}. \quad (11)$$

Here, δ is the fraction of occupied states, i.e., δN_t is the density of charge carriers. B_C is the critical number of bonds per site ($B_C = 2.8$ for a three-dimensional amorphous system) and $\Gamma(z) = \int_0^\infty dy \exp(-y) y^{z-1}$. Equation (11) is calculated assuming (i) that the site positions are random (ii) that hopping takes place between tail states, i.e., δ and T are low (especially $T < T_0$), and (iii) that the energy barrier for the critical hop is large $[\ln(Z_C/Z_0) k_B T \gg k_B T_0]$. The latter criterion means that the tunneling term [first term in Eq. (8)], which decreases drastically for E approaching E_F, forces the system to prefer hops far away from E_F. Equation (11) predicts that the conductivity has an Arrhenius-like temperature dependence in a wide temperature range and that the conductivity increases superlinearly with the density of charge carriers.[1]

To describe the influence of doping, we first assume shallow acceptors in our system, i.e., the acceptor states are below the Fermi level. The term δN_t is then equal to the dopant density N_A and the model predicts a superlinear increase of the conductivity upon doping (as $T < T_0$):

$$\sigma \sim (N_A)^{T_0/T}. \quad (12)$$

Figure 7(a) shows the measured conductivity of the RT samples together with the theoretical curves calculated from Eq. (11). The agreement is quite good. The fit parameters σ_0, α, and T_0 are listed in Table I. Table I also shows the fit parameters for the LT samples, for VOPc and for TDATA, all doped with F_4-TCNQ. TDATA is known as a hole transport material for OLED's.[16] It forms amorphous layers deposited by vacuum evaporation.[28]

In agreement with the results given in[1] for pentacene and PTV (polythienylene vinylene), the main difference between the materials appears not in σ_0 or in the width of the exponential distribution T_0, but in the fit parameter α. The value of α increases from 0.37 Å^{-1} for polycrystalline ZnPc up to 1.39 Å^{-1} for TDATA. The activation energy of the conductivity also increases in this order. As the value of α^{-1} is ≤ 3 Å, i.e., smaller than the size of one molecule, one cannot interpret α^{-1} simply as the Bohr radius, but as an overlap parameter determining the tunneling process.[1] Note that the conductivity data of one material at different doping lev-

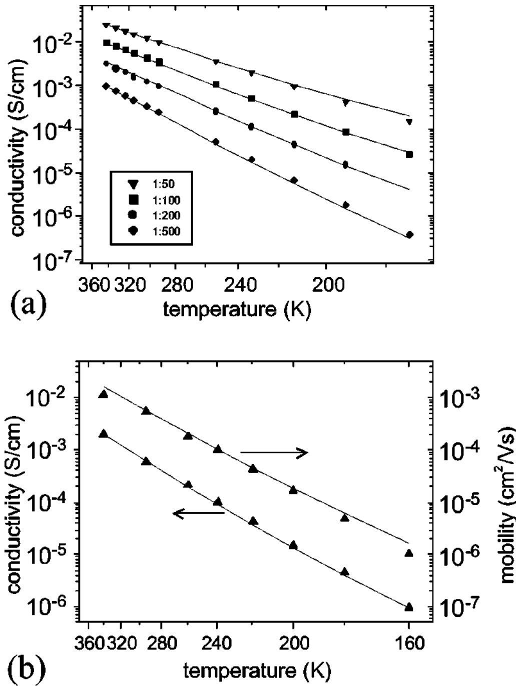

FIG. 7. (a) Conductivity of the RT samples vs temperature. The fit curves are according to Eqs. (11), using $\sigma_0 = 12\times10^5$ S/m, $T_0 = 485$ K and $\alpha = 0.37$ Å^{-1}. (b) Conductivity and field-effect mobility of a RT sample (type I, doping ratio 0.7%) vs temperature. The fit curves are according to Eqs. (11) and (15), using $\sigma_0 = 8\times10^5$ S/m, $T_0 = 500$ K, and $\alpha = 0.4$ Å^{-1}.

els can be modeled with the same values of T_0 and α. This forms a strong indication that the molecular doping does not lead to changes in the layer structure and/or in the energy distribution, i.e., the density of states. We investigated the influence of doping on the morphology for the system ZnPc doped with F_4-TCNQ by electron diffraction. Here, for doping levels up to 5%, no indication for a new crystallographic phase appears.[19]

Among the given materials, ZnPc can be doped best. We can explain this now in the following way: The higher value of α^{-1} is due to a larger overlap of the wave functions. Therefore, the tunneling process is easier and the conductivity higher. In the LT samples, the molecules are less ordered which results in a smaller overlap of the wavefunctions compared to the RT samples. For the different materials, the activation energy of the conductivity increases with decreasing α^{-1}. The reason for this is that for a lower value of α^{-1} tunneling over wide distances is very improbable, so that the charge transport can only take place in an energetic region where the density of states is high, i.e., far away from E_F. Accordingly, the activation energy of the critical hop is high. For each material, the activation energy of the conductivity decreases with increasing dopant concentration which is to be expected according to Eq. (8) as doping shifts E_F closer to an energetic region with high density of states.

TABLE I. Conductivity at 40 °C, activation energy of the conductivity (dopant density 1% for both) and fit parameter σ_0, T_0 and α for polycrystalline ZnPc, amorphous ZnPc (both 30 nm thick layers), VOPc (vanadylphthalocyanine, polycrystalline, 500 nm) and TDATA (4,4′, 4″-tris(N,N-diphenylamino)-triphenylamine, amorphous, 500 nm). Here, σ_0 is a prefactor, T_0 describes the width of the exponential distribution of localized states and α is an overlap parameter determining the tunneling process.

Material	σ(S/cm)	E_{act} (eV)	$\sigma_0(10^5$S/m)	T_0 (K)	α(Å^{-1})
ZnPc (RT)	5.8×10^{-3}	0.18	12 ± 3	485 ± 15	0.37 ± 0.01
ZnPc (LT)	4×10^{-4}	0.23	11 ± 6	455 ± 15	0.64 ± 0.02
VOPc	2.3×10^{-5}	0.32	6 ± 1	485 ± 15	1.00 ± 0.04
TDATA	5.9×10^{-7}	0.34	3 ± 1	515 ± 15	1.39 ± 0.03

We saw that we could describe the doping of several materials by F_4-TCNQ quite self-consistently by assuming shallow acceptors. Nevertheless, we want to see if an equally good description is possible assuming that F_4-TCNQ forms deep acceptor states, i.e., states above E_F the occupation of which is thermally activated. For an exponential distribution of states, a simple calculation using the neutrality equation $p = N_{A^-}$ and Eq. (10) yields

$$p = \delta N_t = (N_t)^{T_0/(T_0+T)}(N_A)^{T/(T_0+T)} \exp\left(\frac{-E_A}{k_B(T_0+T)}\right). \tag{13}$$

Here, N_A and E_A are the density and the LUMO energy level of the acceptor molecules, respectively. For the calculation of $p(E_F)$, the Fermi function was approximated by a step function. Combining Eqs. (11) and (13), we obtain for the conductivity:

$$\sigma(N_A,T) = \sigma_0\left(\frac{\pi(N_t)^{T_0/(T_0+T)}\exp\left(\frac{-E_A}{k_B(T_0+T)}\right)(T_0/T)^3}{(2\alpha)^3 B_C \Gamma(1-T_0/T)\Gamma(1+T_0/T)}\right)^{T_0/T} \times (N_A)^{T_0/(T_0+T)}. \tag{14}$$

Consequently, the conductivity should increase sublinearly upon doping in the case of deep acceptors. Therefore, one can distinguish between deep and shallow dopant states by looking at the behavior of the conductivity upon doping. Within this percolation model, we can conclude that F_4-TCNQ forms shallow acceptor states in any of the materials listed in Table I. At this point a remark should be made about the meaning of the term *shallow acceptors in an exponential distribution of localized states*. In the model of Vissenberg and Matters, a transport level can be defined as the maximum of the differential conductivity $\sigma(E)$, i.e., the main contribution to conductivity comes from the energetic region around this level. The acceptor molecules create extra states at a certain energy level. With increasing (or decreasing) acceptor density the average transport level and the Fermi level shift due to the change in the hole concentration. From our measurements, we can only conclude that the acceptor states are below the Fermi level, i.e., they are occupied with a probability near unity. The energetic distance

between the average transport level and the acceptor level cannot be deduced from our measurements.

To describe the field-effect mobility, we cannot use the equation given by Vissenberg and Matters for μ_{FE} because they assume $p_{ind} \gg p$, where p_{ind} is the induced charge carrier density. Instead of this, we use equation (7) in the form $\mu_{FE} = \triangle\sigma/(ep_{ind})$. The change in the conductivity $\triangle\sigma$ can be developed in linear order:

$$\triangle\sigma \approx \frac{d\sigma}{dp}(p=\delta N_t)p_{ind}, \quad (15)$$

as long as $p_{ind} \ll p$. This linear approximation is justified because our measured transfer characteristics are linear [Fig. 6(a)]. Combining Eqs. (15) and (11), we obtain for the field-effect mobility:

$$\mu_{FE}(\delta,T) = \sigma(\delta,T)\frac{T_0}{T}\frac{1}{e\,\delta N_t}. \quad (16)$$

Figure 7(b) shows the conductivity and the field-effect mobility of a RT sample together with the theoretical curves calculated from Eqs. (11) and (16) assuming shallow acceptor states ($\delta N_t = N_A$). For both curves, the fit parameters are $\sigma_0 = 8\times10^5$ S/m, $T_0 = 500$ K, and $\alpha = 0.4$ Å^{-1}. The values are nearly the same as those in Table I obtained from the conductivity itself. Using a percolation model, we can therefore describe both the conductivity and the field-effect mobility quantitatively in a self-consistent way. In comparison, Schön and Batlogg presented a trapping model for organic thin film field-effect transistors.[31,32] They assume extended states at one transport level and consider the influence of traps (bulk, interface, and grain boundary traps). As shown above, the assumption of one discrete transport level leads to a contradiction for our samples, so we are forced to use a percolation theory both for the polycrystalline and the amorphous samples. Probably, the polycrystalline thin films of pentacene and oligothiophene Schön and Batlogg investigated exhibit a higher degree of order within the microcrystallite than the polycrystalline thin films of ZnPc and VOPc we have investigated here.

Unfortunately, we cannot perform an evaluation of the Seebeck coefficient within this model. The problem is that the percolation theory only considers the critical hopping events, but not the average hops that determine the Seebeck coefficient.

IV. CONCLUSION

We have shown that zinc-phthalocyanine layers can be doped quite efficiently in the polycrystalline and also in the amorphous form by coevaporation with F_4-TCNQ. The amorphous phase can be prepared by evaporating the material onto cooled substrates and is stable up to a temperature of 50 °C. The polycrystalline and the amorphous samples show qualitatively the same electrical behavior: The doping increases the conductivity by up to six orders of magnitude compared to the undoped case and the conductivity increases strongly superlinearly with doping. The (positive) value of the Seebeck coefficient S gets smaller with increasing doping indicating a shift of the Fermi level towards the transport level (using the standard model) and S is temperature independent for all samples. Generally, the conductivity of the amorphous samples is about one order of magnitude lower compared to the polycrystalline samples. The field-effect mobility of the polycrystalline samples is in the order of $10^{-4}-10^{-3}$ cm^{-2}/V s and increases with increasing dopant concentration.

The qualitatively equal electrical behavior of the polycrystalline and the amorphous samples shows that it is very unlikely that the superlinear increase of the conductivity upon doping is caused by high conductance paths or an accumulation of F_4-TCNQ molecules at grain boundaries. Adapting a percolation model presented by Vissenberg and Matters,[1] which assumes hopping transport within a distribution of localized states, we can describe quantitatively the conductivity and the field-effect mobility. The different behavior of polycrystalline ZnPc, amorphous ZnPc, polycrystalline VOPc and amorphous TDATA upon doping can be explained by different values of the overlap parameter α^{-1}, which determines the tunneling process. The superlinear increase of the conductivity upon doping is a strong hint for shallow dopant states as we would expect a sublinear increase for deep dopant states in this model.

Further issues will be to measure the field-effect mobility of the amorphous samples. Moreover, it should be checked if the model is consistent with other electrical measurements such as capacity voltage spectroscopy and current-voltage characteristics of Schottky diodes.

ACKNOWLEDGMENTS

We thank G. Paasch (IFW Dresden) and S. Scheinert (Institut für Festkörperelektronik, TU Ilmenau) for their help concerning the field-effect measurements. We thank the Deutsche Forschungsgemeinschaft (Project No. LE 747/28-1) for financial support.

[1] M.C.J.M. Vissenberg and M. Matters, Phys. Rev. B **57**, 12 964 (1998).
[2] C.W. Tang and S.A. VanSlyke, Appl. Phys. Lett. **51**, 913 (1987).
[3] R.H. Friend, R.W. Gymer, A.B. Holmes, J.H. Burroughes, R.N. Marks, C. Taliani, D.D.C. Bradley, D.A. Dos-Santos, J.L. Bredas, M. Loglund, and W.R. Salaneck, Nature (London) **397**, 121 (1999).
[4] G. Horowitz, Adv. Mater. **10**, 365 (1998).
[5] A.R. Brown, D.M. deLeeuw, E.E. Havinga, and A. Pomp, Synth. Met. **68**, 65 (1994).

[6] C.W. Tang, Appl. Phys. Lett. **48**, 183 (1986).
[7] M. Hiramoto, Y. Kishigami, and M. Yokoyama, Chem. Lett. 119 (1990).
[8] M. Maitrot, G. Guillaud, B. Boudjema, J.J. André, and J. Simon, J. Appl. Phys. **60**, 2396 (1986).
[9] N. El-Khatib, B. Boudjema, G. Guillaud, and M. Maitrot, J. Less-Common Met. **143**, 101 (1988).
[10] B. Boudjema, N. El-Khatib, M. Gamoudi, G. Guillaud, and M. Maitrot, Rev. Phys. Appl. **23**, 1127 (1988).
[11] A. Sussman, J. Appl. Phys. **38**, 27 388 (1967).
[12] A.J. Twarowski, J. Chem. Phys. **76**, 2640 (1982).
[13] J.H. Schön, Ch. Kloc, R.A. Laudise, and B. Batlogg, Phys. Rev. B **58**, 12 952 (1998).
[14] M. Pfeiffer, A. Beyer, B. Plönnigs, A. Nollau, T. Fritz, K. Leo, D. Schlettwein, S. Hiller, and D. Wöhrle, Sol. Energy Mater. Sol. Cells **63**, 83 (2000).
[15] J. Blochwitz, M. Pfeiffer, T. Fritz, and K. Leo, Appl. Phys. Lett. **73**, 729 (1998).
[16] X. Zhou, M. Pfeiffer, J. Blochwitz, A. Werner, A. Nollau, T. Fritz, and K. Leo, Appl. Phys. Lett. **78**, 410 (2001).
[17] A. Nollau, M. Pfeiffer, T. Fritz, and K. Leo, J. Appl. Phys. **87**, 4340 (2000).
[18] M. Pfeiffer, T. Fritz, J. Blochwitz, A. Nollau, B. Plönnigs, A. Beyer, and K. Leo, Adv. Solid State Phys. **39**, 77 (1999).
[19] Martin Pfeiffer, Ph.D. thesis, Dresden, 1999.
[20] P. Görlich, H. G. Schneider, and C. Hamann, *Organische Festkörper und Dünne Schichten* (Akademische Verlagsgesellschaft, Berlin, 1978).
[21] S. Hiller, D. Schlettwein, N.R. Armstrong, and D. Wöhrle, J. Mater. Chem. **8**, 945 (1998).
[22] M. Hoffmann, K. Schmidt, T. Fritz, T. Hasche, V.M. Agranovich, and K. Leo, Chem. Phys. Lett. **258**, 73 (2000).
[23] H. Fritzsche, Solid State Commun. **9**, 1813 (1971).
[24] F. Garnier, G. Horowitz, X.Z. Peng, and D. Fichou, Synth. Met. **45**, 163 (1991).
[25] S. M. Sze, *Physics of Semiconductors Devices* (Wiley, New York, 1981).
[26] C. Clarisse and M.-T. Riou, J. Appl. Phys. **69**, 3324 (1991).
[27] E. A. Silinsh and V. Capek, *Organic Molecular Crystals - Interaction, Localization and Transport Phenomena* (American Institute of Physics, New York, 1994).
[28] Y. Shirota, Y. Kuwabara, H. Inada, T. Wakimoto, H. Nakada, Y. Yonemoto, S. Kawami, and K. Imai, Appl. Phys. Lett. **65**, 807 (1994).
[29] H. Böttger and V. V. Bryskin, *Hopping Conduction in Solids* (Akademie Verlag, Berlin, 1985).
[30] H. Bässler, Phys. Status Solidi B **175**, 15 (1993).
[31] J.H. Schön and B. Batlogg, Appl. Phys. Lett. **74**, 260 (1999).
[32] J.H. Schön and B. Batlogg, J. Appl. Phys. **89**, 336 (2001).